Neutrino Flux Analysis and Monitoring for Power Improvements in NuMI

Nilay Bostan [a], K. Yonehara, L. A. Soplin, A. Wickremasinghe [b], P. Snopok, Y. Yu [c], A. Bashyal [d]

[a]University of Iowa
[b]Fermilab
[c]Illinois Institute of Technology
[d]Oregon State University

Introduction

The determination of the neutrino flux from accelerator neutrino beams exhibits a challenge for the current and future short- and long-baseline neutrino experiments. These experiments provide the measurements of the neutrino oscillation parameters, the mass hierarchy, and the CP phase with high sensitivity. The current flux predictions for the on-axis and off-axis NuMI (Neutrinos at the Main Injector) neutrino detector locations depend on GEANT4 based beam simulation code called G4NuMI. The current simulation uses the new NuMI target, which has 1.5 mm spot size and it is expected to get 900 kW and even more in the upcoming years. In this work, for this new target system, we study the neutrino flux corresponding to the muon energy thresholds seen by the Muon Monitors for FTFP_BERT hadronic model and investigate the neutrino flux predictions at the on-axis and off-axis NuMI neutrino detector locations for FTFP_BERT and QGSP_BERT hadronic models by using G4NuMI beam simulation. We also present the application of the PPFX (Package to Predict the Flux) to the neutrino flux at the on-axis and off-axis NuMI detector locations for FTFP_BERT hadronic model. Finally, we investigate the neutrino spectrum at the NuMI neutrino detector locations that come from π^+ through the focusing components. All plots are based on G4NuMI with 50M protons on target (POT).

A brief description of the NuMI beamline

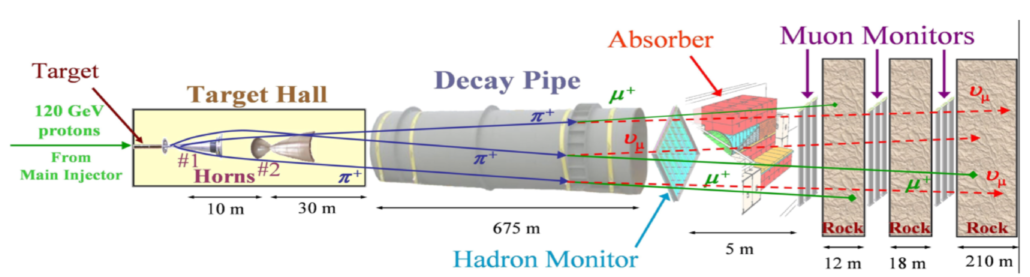

Figure 1: The diagram of the NuMI beamline [1]

- 120 GeV/c momentum protons are delivered by the Fermilab Main Injector (MI). The protons interact with a graphite target to produce mesons — predominantly pions. The pions are focused by a pair of pulsed horn magnets into the decay pipe. The pions then decay to muons and muon neutrinos.
- The Hadron Monitor measures the spatial distribution of the uninteracted protons and undecayed pions, after which they are stopped in the Hadron Absorber.
- The muons penetrate through the absorber and some rock. Their spatial distributions are measured at the three Muon Monitor stations.
- The neutrino beam is unaffected by the rock; the neutrinos propagate forward to detectors.

The comparison between new and old target systems

- New target: 1.5 mm spot size and it is expected to get 900 kW and even more in the upcoming years.
- Old target: 1.3 mm spot size and 700-kW operation.

Neutrino energy and flux

The energy and flux of the neutrinos depend on the decay angle (θ_ν). Assuming that the neutrinos are moving in a near forward direction, for a two-body decay, the neutrino energy can be calculated. The neutrino energy and flux are defined as

$$E_\nu \approx \frac{\left(1-\frac{m_\mu^2}{M^2}\right)E_{\pi(K)}}{1+\gamma^2\tan^2\theta_\nu}, \qquad \Phi_\nu = \left(\frac{2\gamma}{1+\gamma^2\theta_\nu^2}\right)^2\frac{A}{4\pi z^2}, \tag{1}$$

respectively. Here, muon and meson masses are represented by m_μ and M, respectively and E_π, pion parents energy and E_K, kaon parents energy, γ Lorentz boost factor, where $\gamma = \frac{E_{\pi(K)}}{m_{\pi(K)}}$, θ_ν, decay angle between the pions (kaons) and the produced neutrino directions, A, transverse area of the detector and z, the distance between the decay point and the detector locations.

Neutrino flux according to the thresholds of muon energy seen by the Muon Monitors

We show that the neutrino flux for on-axis and off-axis NuMI neutrino detector locations according to the thresholds of muon energy seen by the Muon Monitors (MM). Figures 3, 4 and 5 show that the neutrino spectra for $p + C \to$ any hadron $\to \pi^+ \to \nu_\mu$ (neutrinos from final state pions) interaction for MINERvA and NOvA ND locations by using thresholds for MM1, MM2 and MM3 muons, which are 5, 12 and 22 GeV/c, respectively (it can be seen in figure 2) for FTFP_BERT hadronic model.

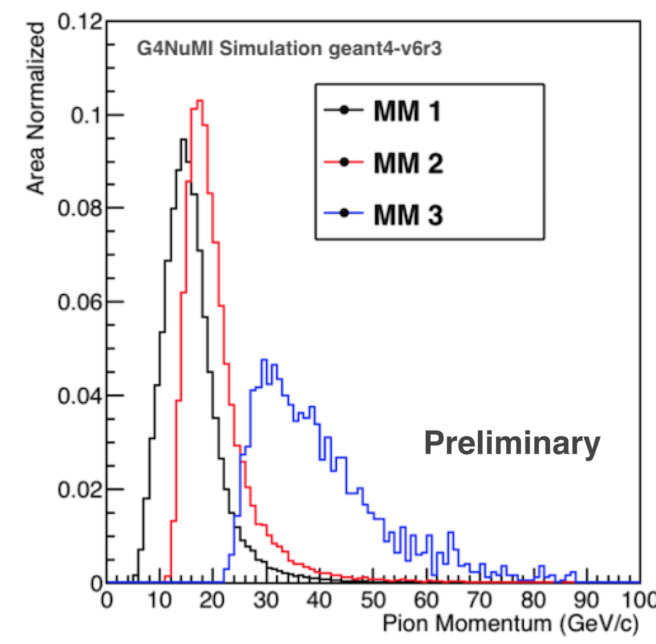

Figure 2: Pion momentum thresholds for MMI, MM2 and MM3. The plot is made by Amit Bashyal.

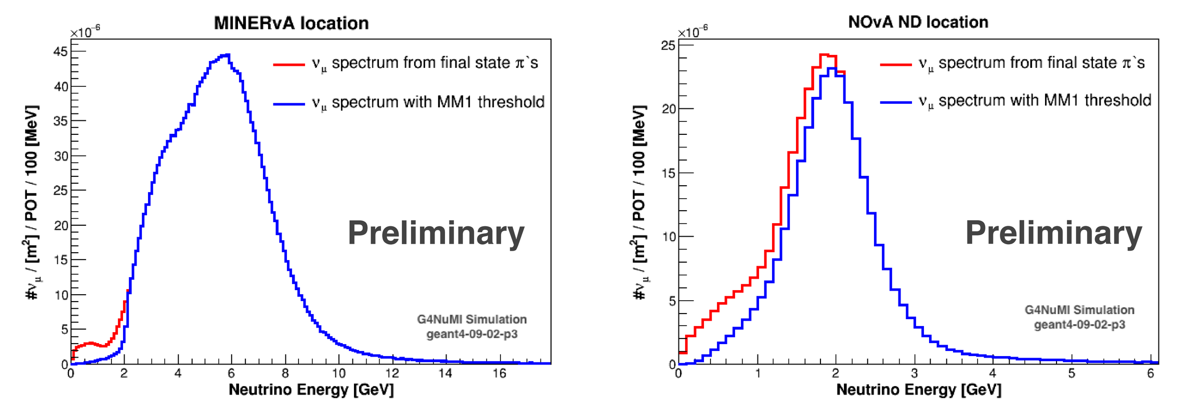

Figure 3: Comparison of neutrino spectrum from final state π's without (red) and with (blue) the MM1 threshold ($P_\pi \geq 5$ GeV/c).

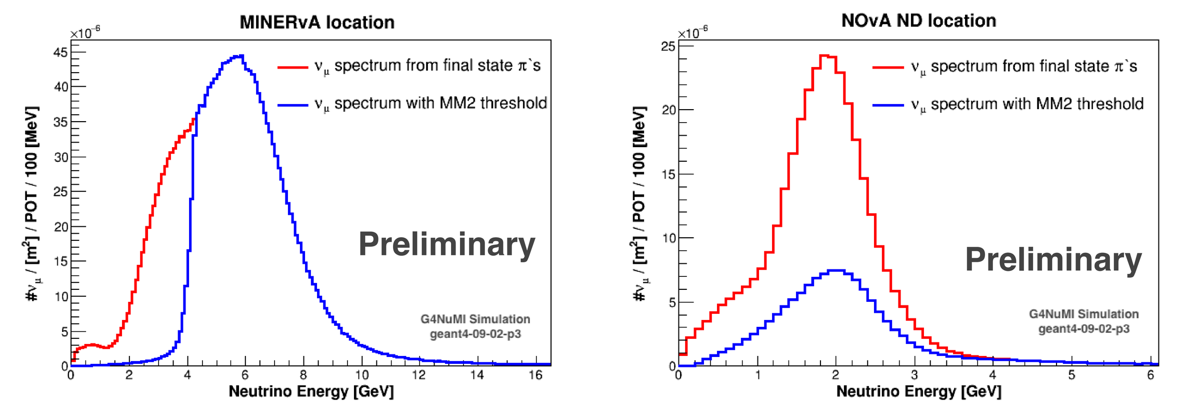

Figure 4: Comparison of neutrino spectrum from final state π's without (red) and with (blue) the MM2 threshold ($P_\pi \geq 12$ GeV/c).

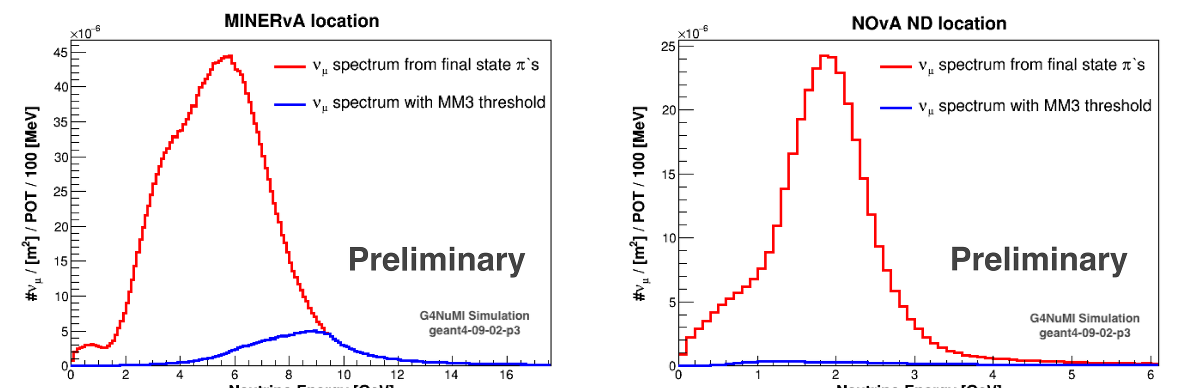

Figure 5: Comparison of neutrino spectrum from final state π's without (red) and with (blue) the MM3 threshold ($P_\pi \geq 22$ GeV/c).

Three muon monitors are located downstream of the hadron absorber (figure 1). Each muon monitor contains 9x9 arrays of ionization chambers. Each ionization chamber consists of two parallel plate electrodes with a gap of 3 mm. The chambers are filled with He gas. Furthermore, muon monitors might help to understand the neutrino flux by looking at the muons, because muons and neutrinos are correlated ($\pi^+ \to \mu^+ + \nu_\mu$). The plots in Figs. 3, 4, 5 show the correlation between the neutrino spectrum and muon monitor energy threshold.

Neutrino spectra at the on-axis and off-axis NuMI neutrino detector locations

Neutrino spectra for $p + C \to \pi^+ \to$ any interaction or decay $\to \nu_\mu$ (secondary pions to final state neutrinos) for FTFP_BERT and QGSP_BERT hadronic models are shown here. Figure 6 shows the results at the MINERvA detector location, figure 7 shows the results at the NOvA ND location. Focusing peak is around 6 GeV for MINERvA and 2 GeV for NOvA ND locations and the ratio between FTFP and QGSP is ≈ 0.9 for MINERvA detector and ≈ 0.85 for NOvA ND locations around focusing peak.

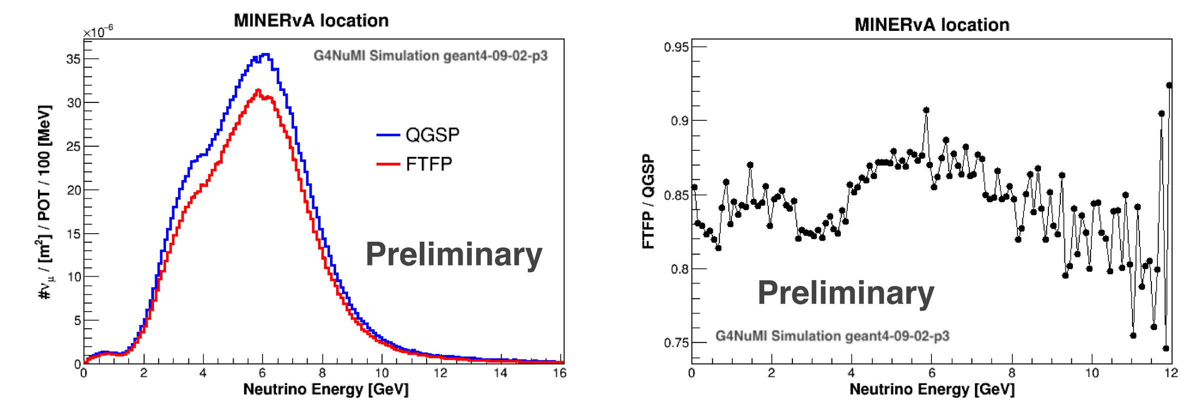

Figure 6: Neutrino spectra for MINERvA detector location.

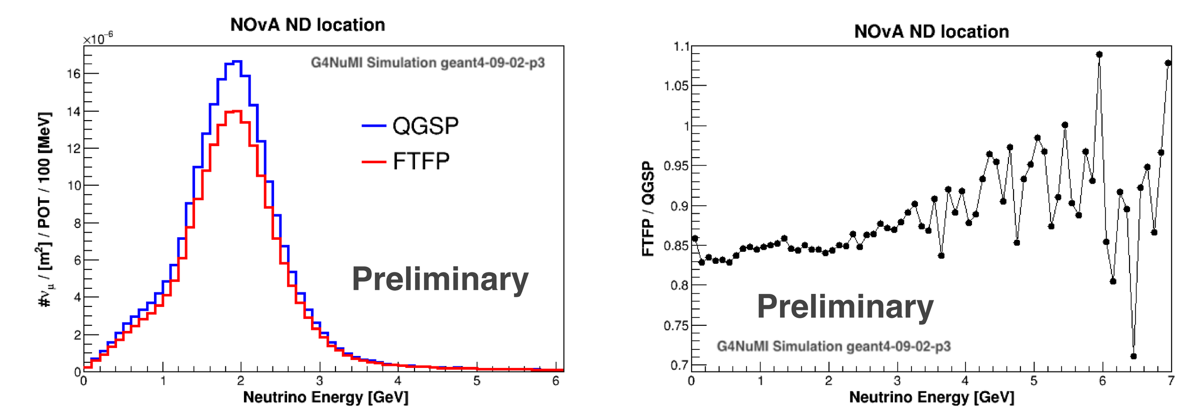

Figure 7: Neutrino spectra for NOvA ND location.

Flux correction by thin target datasets

We compare the impact of hadron production model to external data (NA49) by using PPFX. PPFX corrects and propagates the systematic uncertainties using existing thin target datasets for FTFP_BERT hadronic model with the 'multi-universe' technique applied to a neutrino at an event by event [2]. Figure 8 shows the ratio of PPFX to no PPFX for ν_μ spectra at MINERvA detector and NOvA ND locations. PPFX implies that the value is not nominal (PPFX correction, average flux, central value) in these plots.

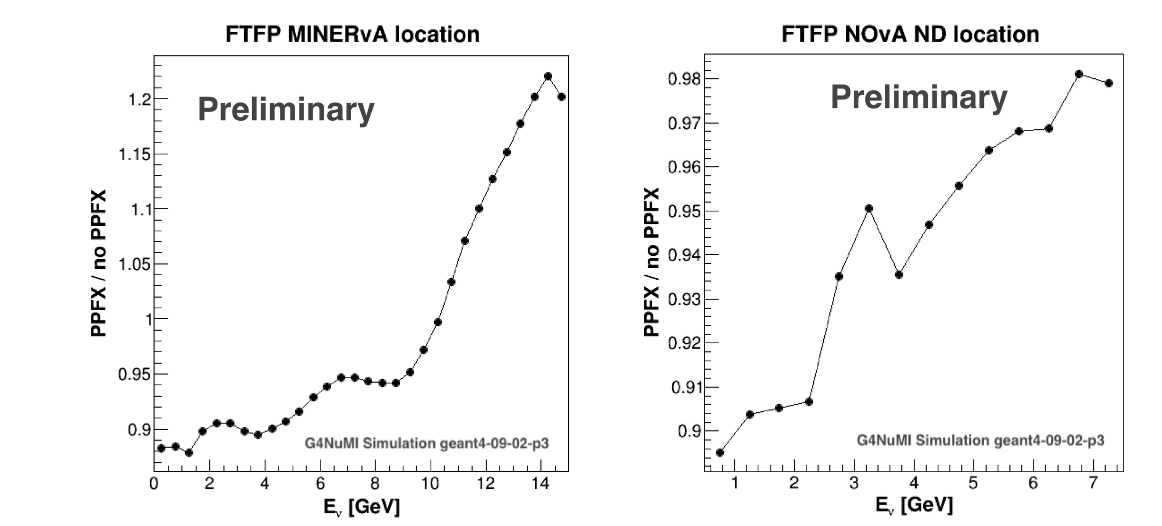

Figure 8: The ratio of PPFX and no PPFX of ν_μ spectra for MINERvA detector and NOvA ND locations.

According to figure 8, the ratio of PPFX to no PPFX for ν_μ spectra ≈ 0.9 both MINERvA detector and NOvA ND locations around focusing peak.

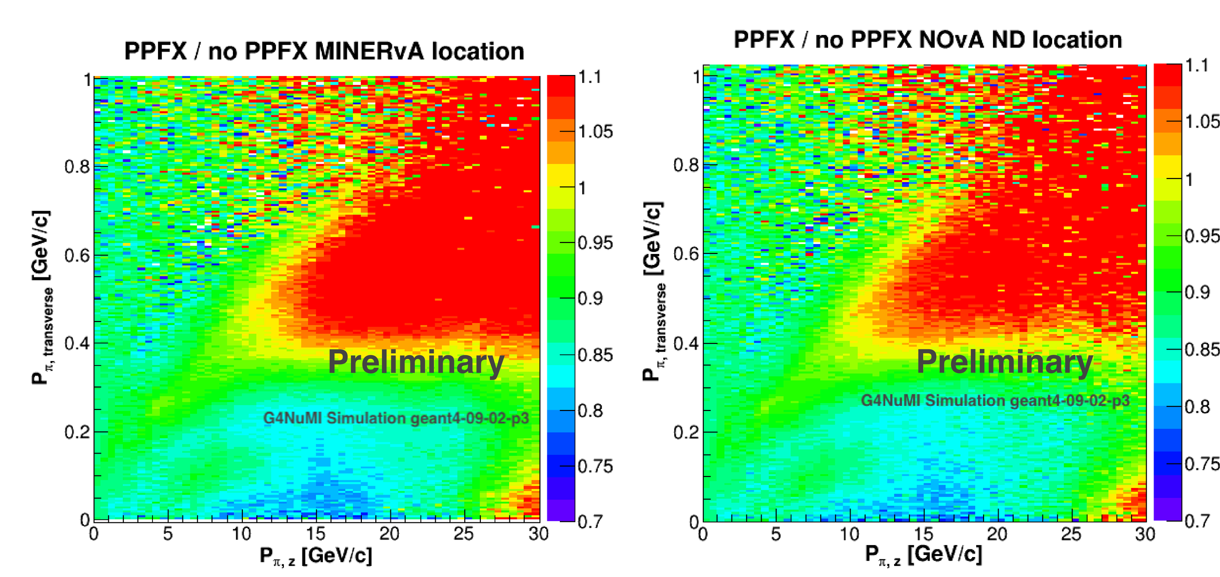

Figure 9: The ratio of PPFX to no PPFX of secondary pions longitudinal momenta vs. transverse momenta distributions.

Figure 9 shows the distribution of the wide range of P_z vs. P_T of secondary pions. For both locations, 10 GeV/c $< P_z <$ 30 GeV/c and $P_T <$ 0.4 GeV/c, the ratio of PPFX to no PPFX is ≈ 0.9. Given the upcoming new data, people would like to extract cross sections for both QGSP and FTFP model and targets and projectiles other than carbon and protons, respectively. We consider that our preliminary results that are given by figures 8 and 9 can help establish relations with these works and our future studies about PPFX.

Focusing components for NuMI new target at NOvA ND and MINERvA locations

We present the focusing components for NuMI, by taking into account the NuMI new target system and FTFP hadronic model at NOvA ND and MINERvA locations. To understand the effect of the focusing system, we split the neutrino flux spectrum into categories (called "focusing components") [2] with respect to how the neutrino parent meson travels from the target through the horns. It depends on the absolute momentum and the relative value of the transverse momentum of the mesons with respect to their longitudinal momentum (figure 10).

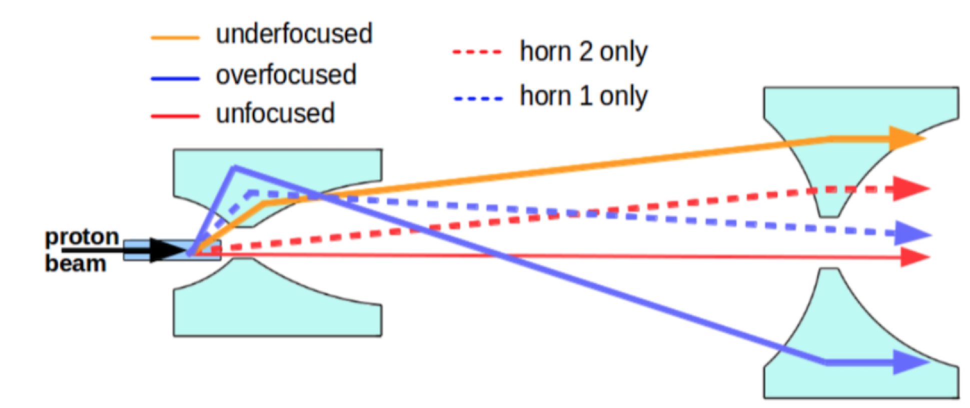

Figure 10: Focusing components with respect to how the neutrino parent meson travels from the target through the horns [2].

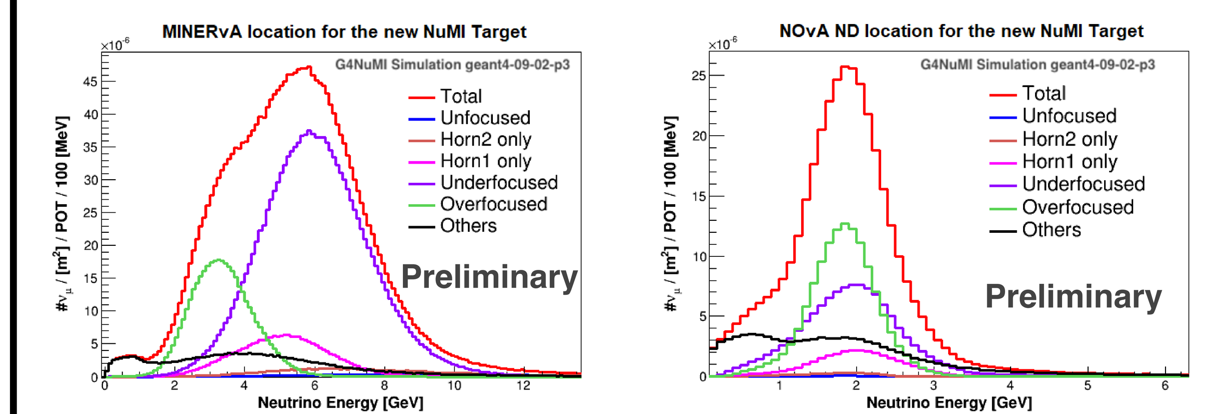

Figure 11: Focusing components of ν_μ that pass through MINERvA and NOvA ND locations for $\pi^+\nu_\mu$ parent.

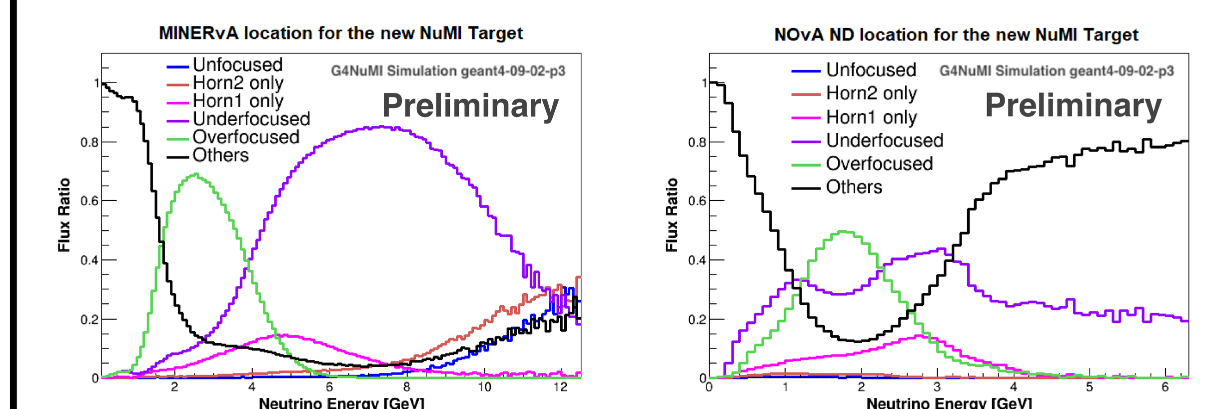

Figure 12: Beam focusing component ratios of ν_μ that pass through MINERvA and NOvA ND locations for $\pi^+\nu_\mu$ parent.

Most of the neutrinos with energies less than 20 GeV have a π^+ parent. If we extend the neutrino energy to 20 GeV for π^+, as we go from higher to lower momentum, unfocused, underfocused and overfocused pion decays populate the ν_μ spectra narrow momentum range values allow the pions to be focused by just one horn. The very low energy neutrinos come mostly from pions born outside of the target ('others') from secondary and tertiary hadrons.

Conclusions

- The NuMI beamline and the new NuMI target are described
- Neutrino flux dependence on the hadronic models at the on-axis and off-axis NuMI neutrino detector locations is shown
- Pion momentum thresholds for MM1, MM2, and MM3 are established at 5, 12 and 20 GeV/c, corresponding neutrino spectra are shown
- QGSP and FTFP models are compared for MINERvA detector and NOvA ND locations
- PPFX correction effects are studied for FTFP model
- Focusing effects were studied for $\pi^+\nu_\mu$ parent using FTFP hadronic model

REFERENCES

[1] Zwaska, Robert Miles. Accelerator systems and instrumentation for the NuMI neutrino beam. United States. doi:10.2172/879065.

[2] Aliaga Soplin, Leonidas. Neutrino Flux Prediction for the NuMI Beamline. United States. doi:10.2172/1250884.

Acknowledgements

NB wish to thank R. Zwaska, J. M. Nachtman and Y. Onel for their contributions and support. This work is supported by DOE Grant No. DE-SC0010113. N. Bostan is also supported by fellowship by Republic of Turkey Ministry of National Education.